Acta Crystallographica Section B
Structural Science
ISSN 0108-7681

Modulated structure of the pseudohexagonal $InFe_{1-x-4\delta}Ti_{x+3\delta}O_{3+x/2}$ (x = 0.61) composite crystal

Yuichi Michiue,[a]* Mitsuko Onoda,[a] Mamoru Watanabe,[a] Francisco Brown[b] and Noboru Kimizuka[b]

[a]Advanced Materials Laboratory, National Institute for Materials Science, 1-1 Namiki, Tsukuba, Ibaraki 305-0044, Japan, and [b]Departamento de Investigaciones en Polimeros y Materiales, Universidad de Sonora, Rosales s/n, Hermosillo, Sonora, CP 83000, Mexico

Correspondence e-mail: michiue.yuichi@nims.go.jp

Received 16 March 2001
Accepted 28 March 2001

The structure of pseudohexagonal-type $InFe_{1-x-4\delta}Ti_{x+3\delta}O_{3+x/2}$ (x = 0.61, δ = 0.04), indium iron titanium oxide, was refined on the basis of a four-dimensional superspace group. The crystal has a compositely modulated structure consisting of two orthorhombic subsystems mutually incommensurate in **b**. The first subsystem $InFe_{1-x-4\delta}Ti_{x+3\delta}O_2$ has a delafossite structure with lattice parameters a = 5.835 (3), b_1 = 3.349 (1) and c = 12.082 (7) Å. The second subsystem with b_2 = 2.568 (6) Å consists of O atoms. The superspace group of the overall structure is $Ccmm(1, 1.305, 0)s00$, which can be converted to $Amam(0, 0, 0.305)0s0$ (No. 63.8). Refinement on 1105 unique reflections converged to R = 0.0303 and wR = 0.0325 with 63 structural parameters. The structure of the first subsystem is the alternate stacking of an edge-shared InO_6 octahedral layer and an Fe/Ti triangle-lattice plane along **c**. A sheet of O atoms in the second subsystem is also extending on the Fe/Ti plane, where displacive modulation of atoms is prominent.

1. Introduction

In recent synthetic studies in the pseudobinary system $InFeO_3$–$In_2Ti_2O_7$ (Brown, Flores *et al.*, 1999) two phases were obtained. The phases have much flexibility in chemical species and isostructural compounds are obtained in systems In_2O_3–TiO_2–M_2O_3 (M = Al, Ga, Cr, Fe) and In_2O_3–TiO_2–$M'O$ (M' = Mg, Mn, Co, Ni, Cu, Zn; Brown, Kimizuka *et al.*, 1999; Kimizuka *et al.*, 2000; Brown *et al.*, 2001). All compounds of the family give diffraction patterns with a set of strong reflections accompanying weak satellites at commensurate ($b^*/3$) or incommensurate positions. From X-ray diffraction analyses based on main reflections only it has been clarified that the phase formed in an Fe-rich region ($InFeO_3/In_2Ti_2O_7 > 1$ at 1373 K) has a pseudohexagonal structure (Michiue *et al.*, 1999), and the other one in a Ti-rich region ($InFeO_3/In_2Ti_2O_7 \leq 1$ at 1373 K) is a pseudorhombohedral type (Michiue *et al.*, 2000). The pseudohexagonal type is closely related to $InFeO_3$ (Giaquinta *et al.*, 1994) with hexagonal symmetry. The pseudorhombohedral form is a stacking variant of the pseudohexagonal form. The $InFeO_3$ structure is characterized by alternate stacking of two layers along **c**; one is an edge-shared InO_6 octahedral sheet and the other consists of FeO_5 trigonal bipyramids. This can be regarded as a stuffed delafossite structure (Prewitt *et al.*, 1971). Fe atoms are partially replaced by Ti atoms in the pseudohexagonal-type structure and concomitantly excess O atoms are introduced into the Fe/Ti—O layer to keep charge neutrality of the whole crystal. The arrangement of O atoms in this layer was approximated by the partial occupation at a honeycomb lattice (Michiue *et al.*,

1999). Large thermal parameters U^{11} and U^{22} for oxygen ions on the Fe/Ti—O plane, however, suggested the prominent displacement of the atoms. Observation of satellite reflections implies that such displacements are not random, but to be definitely described by modulation functions. Coordination features around the Fe/Ti can be clarified only by an analysis including satellite reflections. In this study a superspace-group approach was applied for the pseudohexagonal-type crystal. It has been found that the structure is properly described as a composite crystal consisting of two subsystems, although the scattering ability of the second subsystem is so weak that main reflections of the second subsystem are almost comparable in strength to satellites.

2. Experimental

A single-crystal grown by a slow cooling method (Brown, Kimizuka *et al.*, 1999) was mounted on an automated four-circle diffractometer (Rigaku AFC-7*R*). Conditions and parameters for data collection and refinement are listed in Table 1.[1] Two orthorhombic unit cells with common a and c parameters are used for indexing the reflections. The two subsystems are mutually incommensurate in **b**. Lattice parameters a = 5.835 (3), b_1 = 3.349 (1) and c = 12.082 (7) Å are determined by 25 main reflections ($52.1 < 2\theta < 54.3^\circ$) of the first subsystem and b_2 = 2.567 (8) Å determined by 25 reflections ($20.2 < 2\theta < 48.7^\circ$) of the second. The superspace group of the overall structure is $Ccmm(1, 1.305, 0)s00$, where the modulation wavevector is $\mathbf{q} = \mathbf{a}^* + \mathbf{b}_2^* = \mathbf{a}^* + 1.305\mathbf{b}_1^*$ and the $\boldsymbol{\sigma}$ vector (σ_1, σ_2, σ_3) defined by $\mathbf{q} = \sigma_1\mathbf{a}^* + \sigma_2\mathbf{b}_1^* + \sigma_3\mathbf{c}^*$ is (1, 1.305, 0). Symmetry operations based on a conventional basis ($\mathbf{a}^*$, $\mathbf{b}_1^*$, $\mathbf{c}^*$, $\mathbf{q}^i = \sigma_2\mathbf{b}_1^* = \mathbf{b}_2^*$) are $(0, 0, 0, 0; \frac{1}{2}, \frac{1}{2}, 0, \frac{1}{2}) + x_1, x_2, x_3, x_4$; $x_1, x_2, \frac{1}{2} - x_3, x_4$; $x_1, -x_2, x_3, \frac{1}{2} - x_4$; $x_1, -x_2, \frac{1}{2} - x_3, \frac{1}{2} - x_4$; $-x_1, -x_2, -x_3, -x_4$; $-x_1, -x_2, \frac{1}{2} + x_3, -x_4$; $-x_1, x_2, -x_3, \frac{1}{2} + x_4$; $-x_1, x_2, \frac{1}{2} + x_3, \frac{1}{2} + x_4$. This superspace group can be converted to $Amam(0, 0, 0.305)0s0$ (No. 63.8; Janssen *et al.*, 1999) by $\mathbf{a}'^* = \mathbf{c}^*$, $\mathbf{b}_1'^* = \mathbf{a}^*$, $\mathbf{c}'^* = \mathbf{b}_1^*$, $\mathbf{q}' = \mathbf{q}^i - \mathbf{b}_1^*$. Reciprocal base vectors of the two subsystems ($\mathbf{a}^*$, $\mathbf{b}_1^*$, $\mathbf{c}^*$) and ($\mathbf{a}^*$, $\mathbf{b}_2^*$, $\mathbf{c}^*$) are related to the conventional basis in four-dimensional reciprocal space ($\mathbf{a}^*$, $\mathbf{b}_1^*$, $\mathbf{c}^*$, $\mathbf{b}_2^*$) through Z matrices (Janner & Janssen, 1980).

$$Z^1 = \begin{pmatrix} 1 & 0 & 0 & 0 \\ 0 & 1 & 0 & 0 \\ 0 & 0 & 1 & 0 \end{pmatrix} \qquad \text{(Subsystem 1)}$$

$$Z^2 = \begin{pmatrix} 1 & 0 & 0 & 0 \\ 0 & 0 & 0 & 1 \\ 0 & 0 & 1 & 0 \end{pmatrix} \qquad \text{(Subsystem 2)}$$

The indexing by $h\mathbf{a}^* + k\mathbf{b}_1^* + l\mathbf{c}^* + m\mathbf{b}_2^*$ showed systematic reflection conditions $h + k + m = 2n$ for $hklm$ and $l + m = 2n$ for $0klm$ (n: integer). The former is due to the centering translation $(\frac{1}{2}, \frac{1}{2}, 0, \frac{1}{2})$ and the latter is by the hyper n-glide plane; $-x_1$, x_2, $\frac{1}{2} + x_3$, $\frac{1}{2} + x_4$.

[1] Supplementary data for this paper are available from the IUCr electronic archives (Reference: SN0010). Services for accessing these data are described at the back of the journal.

Table 1
Crystallographic data and conditions for data collection and refinement.

Mr	215.5
Crystal system	Orthorhombic
Superspace group	$Ccmm(1, 1.305, 0)s00$
a (Å)	5.835 (3)
b_1 (Å)	3.349 (1)
c (Å)	12.082 (7)
b_2 (Å)	2.568 (6)
V (Å^3)	236.1 (2)
Z	4
D_x (g cm^{-3})	6.062
μ(Mo $K\alpha$) (mm^{-1})	13.2
Crystal size (mm)	0.13 × 0.28 × 0.03
Color	Brown
Radiation	Mo $K\alpha$ (0.71069 Å)
Monochromator	Graphite
Scan mode	ω–2θ
$2\theta_{max}$ (°)	90
h, k, l, m range	$-11 \le h \le 11$
	$-2 \le k \le 10$
	$-24 \le l \le 24$
	$-4 \le m \le 4$
Standard reflections	3 every 200
No. of reflections measured	13 423
All/unique reflections with $F_o > 3\sigma(F_o)$	4113/1105
Absorption correction	Analytical
Transmission factor	0.052–0.603
Extinction correction	Isotropic
R, wR	
all reflections	0.0303, 0.0325
main reflections of subsystem 1 ($m = 0$)	0.0205, 0.0292
No. of reflections	345
main reflections of subsystem 2 ($k = 0$)	0.0318, 0.0376
No. of reflections	164
common main reflections ($k = m = 0$)	0.0250, 0.0363
No. of reflections	68
satellite reflections ($m \neq 0, k \neq 0$)	0.0487, 0.0511
No. of reflections	664

A program for the least-squares refinement of modulated structures *REMOS*90 (Yamamoto, 1992) was used. Fractional coordinates and thermal parameters for atoms in the jth subsystem are given by

$$u_j = u_{j0} + A_0 + \sum_{n>0}[A_n \cos(2\pi nt) + B_n \sin(2\pi nt)],$$

where $t = \mathbf{q}_j^i(\mathbf{n}_j + \mathbf{r}_j)$, $\mathbf{n}_j$ is the lattice vector, $\mathbf{r}_j$ the position of the fundamental structure (a_jx_{j0}, b_jy_{j0}, c_jz_{j0}). A_0, A_n and B_n are refined parameters. Restrictions for Fourier coefficients of modulation functions for atoms at special positions were obtained by programs *SPA*, *SPL* and *SPT* (Kato & Onoda, 1991, 1992). Fourier coefficients up to fourth-order have been taken into account for positional parameters of all atoms, although coefficients higher than second-order of the O atom in the first subsystem had no significant values and fixed to 0. Coefficients of thermal parameters for metal sites were refined up to second order, while no modulation was considered for the thermal parameters of O atoms.

3. Refinement

The final structural parameters are listed in Table 2. The first subsystem consists of In, Ti, Fe and some of the oxygen ions, O1, while the remaining O atoms, O2, construct the second

Table 2
Structural parameters.

Temperature factors take the form $\exp\{-(h^2\beta_{11} + k^2\beta_{22} + l^2\beta_{33} + 2hk\beta_{12} + 2hl\beta_{13} + 2kl\beta_{23})\}$; $B_{eq} = (4/3)\Sigma_i\Sigma_j\beta_{ij}a_ia_j$.

	x	y	z	Occ.
Subsystem 1				
In	0	0	0	
A_0	0	0	0	1
A_1	0	0	0	
B_1	−0.01854 (7)	0	0.00102 (4)	
A_2	0	0	0	
B_2	0	−0.0003 (3)	0	
A_3	0	0	0	
B_3	0.0009 (4)	0	0.0006 (2)	
A_4	0	0	0	
B_4	0	0.007 (1)	0	
M(Fe/Ti)	0.33	0	0.25	
A_0	0.004 (1)	0	0	0.23 (1)/0.73 (1)
A_1	0	−0.0063 (7)	0	0
B_1	−0.0468 (5)	0	0	0.07 (2)/−0.06 (2)
A_2	−0.0005 (7)	0	0	−0.28 (3)/0.21 (3)
B_2	0	−0.021 (1)	0	0
A_3	0	−0.004 (2)	0	
B_3	0.004 (1)	0	0	
A_4	−0.001 (1)	0	0	
B_4	0	−0.016 (3)	0	
O1	0.33	0	0.086	
A_0	0.0017(5)	0	−0.0009 (2)	1
A_1	0	−0.000 (1)	0	
B_1	−0.0273 (6)	0	0.0006 (3)	
A_2	−0.002 (1)	0	−0.0006 (5)	
A_2	−0.002 (1)	0.001 (2)	0	
Subsystem 2				
O2	0.08	0.25	0.25	
A_0	0.001 (2)	0	0	1
A_1	−0.144 (1)	0	0	
B_1	0	−0.021 (6)	0	
A_2	0.008 (3)	0	0	
B_2	0	−0.098 (4)	0	
A_3	0.008 (3)	0	0	
B_3	0	0.007 (8)	0	
A_4	0.003 (4)	0	0	
B_4	0	0.062 (7)	0	

	β_{11}	β_{22}	β_{33}	β_{12}	β_{13}	β_{23}	B_{eq}
Subsystem 1							
In							
A_0	0.00333 (4)	0.0096 (2)	0.00154 (1)	0	−0.00005 (2)	0	0.593 (4)
A_1	0	0	0	−0.0008 (1)	0	0.00061 (7)	0.000 (0)
B_1	0	0	0	0	0	0	0
A_2	0.0005 (2)	0.0006 (5)	0.00009 (3)	0	0.00002 (6)	0	0.05 (1)
B_2	0	0	0	0	0	0	
M							
A_0	0.0095 (3)	0.034 (2)	0.00081 (3)	0	0	0	1.09 (3)
A_1	0	0	0	0.0030 (7)	0	0	0.000 (0)
B_1	−0.0026 (5)	0.015 (2)	0.00006 (7)	0	0	0	0.12 (5)
A_2	0.0011 (8)	−0.014 (3)	0.0001 (1)	0	0	0	−0.15 (6)
B_2	0	0	0	0.004 (1)	0	0	0.000 (0)
O1							
A_0	0.0045 (4)	0.014 (1)	0.00089 (8)	0	0.0000 (2)	0	5.9 (3)
Subsystem 2							
O2							
A_0	0.018 (2)	0.08 (1)	0.0014 (2)	0	0	0	1.7 (1)

subsystem. Fundamental structures of the two subsystems have space group *Ccmm*, although the origin of the second subsystem is displaced by (1/4, 1/4, 0). Namely, the 8(*d*) site, the inversion center, of the second subsystem is put on the 4(*a*) site, the origin on 2/*m*, of the first subsystem. The first subsystem $InFe_{1-x-4\delta}Ti_{x+3\delta}O_2$ basically has a delafossite structure (Prewitt *et al.*, 1971), which is the alternate stacking of an edge-shared InO_6 octahedral layer and a triangle-lattice plane of the *M* site occupied by Fe and Ti atoms along **c**. The *M* and O1 atoms form a linear coordination O1—*M*—O1 nearly along **c**. The second subsystem consists of an oxygen (O2) sheet extending on the *M*-site plane. The overall structure is characterized as an alternate stacking of the $InO1_6$ octahedral layer and the *M*—O2 sheet along **c**.

Occupational modulation at the *M* site, which is an important factor for the interpretation of the coordination feature, was carefully examined. Inhomogeneity in the product of the crystal growth prevented us from obtaining the precise composition by the chemical analysis. At early stages of the refinement, no vacancy was considered at the *M* site. The occupation ratio Fe/Ti, initially set to 0.39/0.61 (R = 0.376, wR = 0.382) to keep the charge neutrality of the whole crystal, was refined to give the value 0.09/0.91 (R = 0.318, wR = 0.337). This result is improbable because of the following reasons.

(i) There is no possible mechanism to compensate excess positive charges caused by the considerable decrease in the Fe^{3+}/Ti^{4+} ratio. Introduction of vacancies at the In site was ruled out by the refinement of the occupation ratio at the In site. It seems impossible to

introduce additional oxygen ions in the $InO1_6$ layer and the M—O2 sheet.

(ii) Succeeding refinement for modulation of the occupation ratio at the M site resulted in values exceeding the limit of the possible range. Namely, Ti occupation ratio reached 1.39 with the Fe ratio −0.39 in some parts of the structure.

(iii) The Fe/Ti ratio in the starting mixture of the crystal growth was 1/2, and the ratios about 1/4 were given from EPMA measurements of a few crystals obtained along with the crystal used for the data collection. The refined Fe/Ti ratio, *ca.* 1/10, is far less than these values.

Thus, it is assumed that there are some vacancies at the M site in order to decrease the amount of electrons at the site. In addition, the full occupation at the O2 site was assumed because the second subsystem is merely the sheets of O2 atoms and the removal of some of the O2 atoms will cause the rearrangement of the atoms giving the less concentrated O2 sheet with the larger b_2. (On the other hand, vacancies at the M sites cause no change in the periodicity of the first subsystem, because the structure of the first subsystem is three-dimensionally connected.) This assumption leads to a relation between the chemical composition and σ_2. Namely, the positive charge of the first subsystem should be $2\sigma_2$. As the complete $InO1_6$ octahedral sheet (InO_2^-) is concluded in the present study, the triangular lattice of the M should have the charge $1 + 2\sigma_2$ ($= 1 + 2 \times 1.305 = 3.61$). Thus, a constraint was imposed on occupation ratios of Fe and Ti in the refinement; $3A_0(\mathrm{Occ_{Fe}}) + 4A_0(\mathrm{Occ_{Ti}}) = 3.61$. The values obtained in Table 2 give the nominal composition In $\mathrm{Fe}_{1-x-4\delta}\mathrm{Ti}_{x+3\delta}\mathrm{O}_{3+x/2}$ ($x = 0.61$, $\delta = 0.04$), including 4% vacancies at the M site. At the next step, that is the refinement of modulation functions for occupation ratios, there is a problem of strong correlation between the occupation ratios of Fe and Ti, which can be independently refined because of the M site vacancies. First, no modulation was assumed for the vacancy and the modulation of the Fe/Ti ratio was refined with constraints $B_1(\mathrm{Occ_{Fe}}) + B_1(\mathrm{Occ_{Ti}}) = 0$ and $A_2(\mathrm{Occ_{Fe}}) + A_2(\mathrm{Occ_{Ti}}) = 0$. Parameters obtained gave unrealistic compositions in parts. Around $t = 0$, the occupation ratio was 1.22 for Ti and −0.26 for Fe, which suggests that the amount of electrons should be less than that of the complete substitution of Ti for Fe, *i.e.* 96% Ti and 4% vacancy. Such a condition is realised by considering the modulation of the vacancy concentration. Thus, new constraints $\alpha B_1(\mathrm{Occ_{Fe}}) + B_1(\mathrm{Occ_{Ti}}) = 0$ and $\alpha A_2(\mathrm{Occ_{Fe}}) + A_2(\mathrm{Occ_{Ti}}) = 0$ ($\alpha > 1$) were imposed, where the modulation of the vacancy is given by $(\alpha - 1)\{B_1(\mathrm{Occ_{Ti}})\sin 2\pi t + A_2(\mathrm{Occ_{Ti}})\cos 4\pi t\}$. From refinements with various α, it has been found that small α leads to the negative Fe occupation ratio around $t = 0$, while large parameters give the negative content of the vacancy around $t = 1/4$ (this means the summation of Ti and Fe exceeds unity). To avoid such unrealistic compositions, the parameter was set to 1.3 as a moderate value. Slightly negative occupancies still appeared for the Fe and the vacancy as shown in Fig. 1, but we took the result as acceptable by considering estimated errors of the Fourier coefficients.

Displacive modulation functions for x and y are shown in Fig. 1. Modulations along **c** are forbidden for M and O2 and

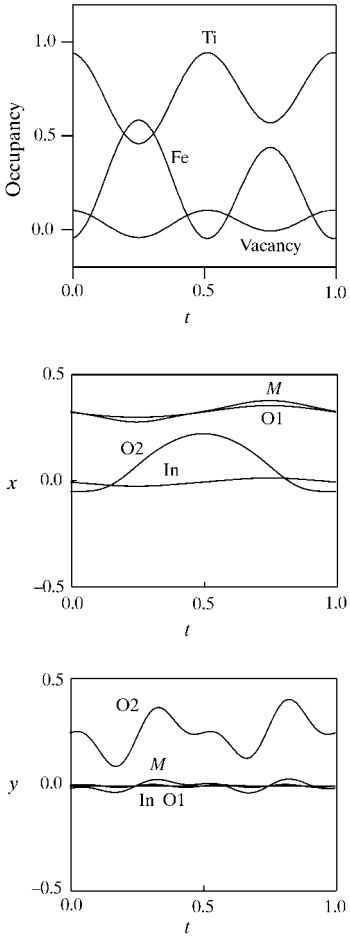

Figure 1
Occupational and displacive modulation functions. Displacive modulations along **c** are forbidden or negligible.

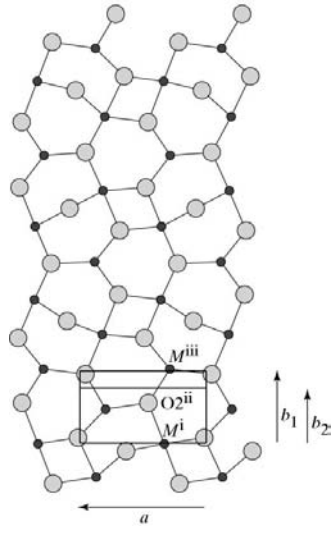

Figure 2
Coordination between metal (Fe/Ti) and oxygen atoms on the plane $z = 1/4$. Small and large circles represent metal and oxygen atoms, respectively. Metal–oxygen pairs within 2.1 Å are indicated by lines.

almost negligible for In and O1. The most prominent displacements are seen for the O2 atom on the $z = 1/4$ plane because the triangular lattice of M belonging to the first subsystem is on the same plane (Fig. 2). The interatomic distance between M and O2 is given as a function of t' ($= -\sigma_2 x_2 + x_4$) in Fig. 3. If the atoms suffer no modulation, as given by the dotted line, $O2^{i}$ and $O2^{ii}$ are within 1.5 Å of M^{i} at around $t' = 0.25$ and 0.75, respectively. The values are too short for distances between a metal (Fe or Ti) and an oxygen ion because the ionic radius is 0.645 Å for Fe^{3+}, 0.605 Å for Ti^{4+} (in six coordination) and 1.40 Å for O^{2-} (Shannon, 1976). In the modulated structure the M—O2 distance always exceeds 1.74 Å, which is, however, still short judging from ionic radii. O2—O2 distances given in Fig. 4 take 2.31 Å as the shortest one. The value is also a little too short, despite the fact that similarly short O—O distances are seen in some compounds such as T-Nb_2O_5 containing pentagonal bipyramidal coordinations [O—O distance: 2.32 (3), 2.34 (2) Å *etc*.; Kato & Tamura, 1975]. These facts suggest that displacive modulations given by a Fourier series up to fourth order are insufficient to give correct atomic positions, especially for the strongly modulated O2 atom. Refinements with higher Fourier terms were, however, unsuccessful, giving the shorter M—O2 and O2—O2 distances in parts. This is probably because the scattering ability of O is far less than those of In, Fe and Ti. Superspace groups with the lower symmetry, which allow displacive modulations for M and O2 atoms along z, were not adopted, because modulation amplitudes were so small as to improve little the short interatomic distances and no significant improvement was seen in reliability factors by refinements based on such superspace groups. The primary origin of the modulation in this sheet is undoubtedly the repulsive interaction between the metal and oxygen atoms. This problem is again discussed in §4.

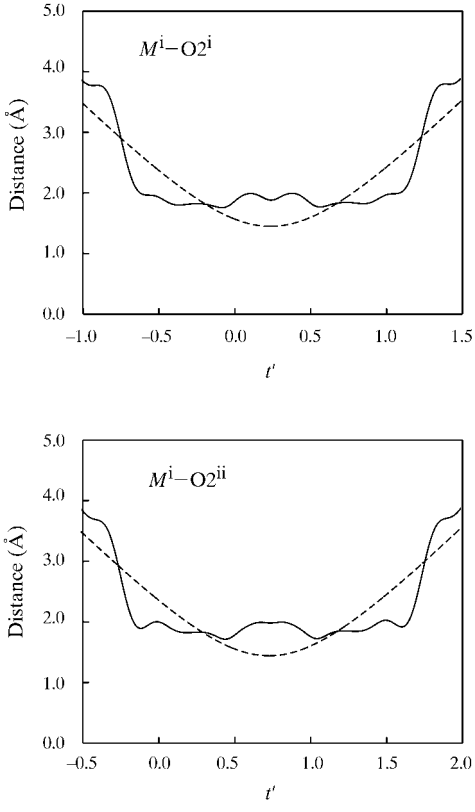

Figure 3
M—O2 distances as functions of t' ($= -\sigma_2 x_2 + x_4$). Solid and dotted lines represent modulated and unmodulated structures, respectively. M^{i}, $O2^{i}$ and $O2^{ii}$ atoms correspond to those in Fig. 2. Symmetry operations are (i) x_1, x_2, x_3, x_4; (ii) $x_1 + \frac{1}{2}, x_2 + \frac{1}{2}, x_3, x_4 + \frac{1}{2}$.

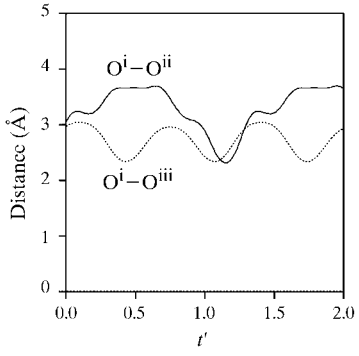

Figure 4
O2—O2 distances as functions of t' ($= -\sigma_2 x_2 + x_4$). Symmetry operations are (i) x_1, x_2, x_3, x_4; (ii) $x_1 + \frac{1}{2}, x_2 + \frac{1}{2}, x_3, x_4 + \frac{1}{2}$; (iii) $x_1, x_2 + 1, x_3, x_4$.

4. Discussion

Definite determination of the coordination number is impossible for many of the M sites in Fig. 2, because the inclusion of an O atom in the coordination may be arbitrary when an atom is at an intermediate distance from the metal site. The number of O2 atoms within a given distance from the M site is obtained from Fig. 5, which shows distances of O2 atoms from M^{i}. The figure shows that if 2.1 Å is taken as a limit of M—O2 coordination, a metal ion with $t' = 0$ is coordinated by four O2 ions. The total coordination number of this metal site is 6 including two M—O1 bonds approximately normal to the M—

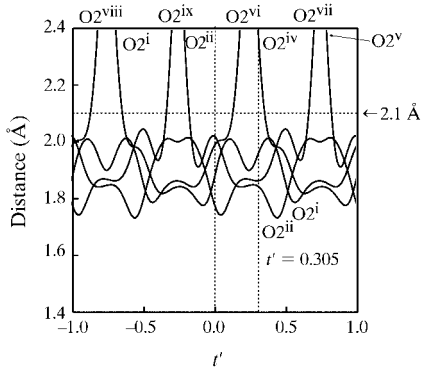

Figure 5
Variation of the coordination feature of the M site as functions of t' ($= -\sigma_2 x_2 + x_4$). Coordination environments at $t' = 0$ and 0.305 indicated by dotted lines are equivalent to those of the M^{i} and M^{iii} in Fig. 2, respectively. Symmetry operations are (i) x_1, x_2, x_3, x_4; (ii) $x_1 + \frac{1}{2}, x_2 + \frac{1}{2}, x_3, x_4 + \frac{1}{2}$; (iii) $x_1, x_2 + 1, x_3, x_4$; (iv) $x_1, x_2, x_3, x_4 + 1$; (v) $x_1 + \frac{1}{2}, x_2 + \frac{1}{2}, x_3, x_4 + \frac{3}{2}$; (vi) $x_1, x_2, x_3, x_4 - 1$; (vii) $x_1 + \frac{1}{2}, x_2 + \frac{1}{2}, x_3, x_4 - \frac{1}{2}$; (viii) $x_1, x_2, x_3, x_4 - 2$; (ix) $x_1 + \frac{1}{2}, x_2 + \frac{1}{2}, x_3, x_4 - \frac{3}{2}$.

O2 plane. Another metal ion with $t' = 0.305$, for example, is regarded as a five-coordination site, because only three O2 atoms are found within the limit. These coordination environments at $t' = 0$ and 0.305 correspond to M^{i} and M^{iii} in Fig. 2, respectively. The coordination number for the M site based on the limit distance of 2.1 Å is five or six, which are repeated alternately according to the variation of t'.

The variation of the coordination feature is associated with the occupational ordering of metal ions, Fe and Ti, at the M site in Fig. 1. The site is mostly occupied by Ti with ∼10% vacancy in six coordination regions around $t' = 0$ and 0.5. (Note that $t = t'$ for M.) By considering the trigonal bipyramidal coordination of Fe in $InFeO_3$ (Giaquinta *et al.*, 1994) it is reasonable to assume that the Fe ratio increases to ∼60 and 40% in five coordination regions around $t' = 0.25$ and 0.75, respectively, although the rest are Ti atoms. Five-coordination is rather uncommon for Ti, but the trigonal bipyramid around Ti is seen in La_2TiO_5 (Guillen & Bertaut, 1966) and In_2TiO_5 (Senegas *et al.*, 1975).

It is expected that the variation of the coordination feature is correlated to the variation of the bond-valence sum (BVS) at the M site. The estimation of the r_0 parameter for the calculation of BVS is, however, difficult because three species, Fe, Ti and vacancy, should be considered at the site. Ignoring the vacancy, composition-weighted means at a given t', $r_0(t') = \{Occ_{Ti}(t')r_0(Ti^{4+}) + Occ_{Fe}(t')r_0(Fe^{3+})\}/\{Occ_{Ti}(t') + Occ_{Fe}(t')\}$, is used in Fig. 6, where $r_0(Ti^{4+}) = 1.815$ and $r_0(Fe^{3+}) = 1.759$ Å (Brown & Altermatt, 1985). The tendency is generally as expected; the BVS varies according to the Ti^{4+}/Fe^{3+} ratio. In the lower coordination regions around $t' = 0.25$ and 0.75, the calculated BVS is close to 3.5, as expected from roughly comparable occupation ratios of Fe^{3+} and Ti^{4+}. The BVS, however, exceeds the limit, 4, in the higher coordination regions around $t' = 0$ and 0.5, where the site is mostly occupied by Ti^{4+}. One of the possible reasons for high BVS is that vacancies were ignored in the BVS calculation. A cation vacancy usually causes the elongation of distances between anions surrounding the cation site. However, the opposite change may happen in dense structures like the present compound. It is probable that actual Ti—O2 distances are longer than M—O2 distances.

Another reason for abnormally high BVS in parts might be that Fourier terms up to fourth order are insufficient for modulation functions to give the precise positions of atoms. Trajectories of $O2^{i}$ and $O2^{ii}$ atoms on the plane $z = 1/4$ are plotted in Fig. 7, where fractional coordinates x and y (based on b_2) are given as functions of t' ($-2 \le t' \le 2$). M sites without modulations, which form a triangular lattice, are also shown in Fig. 7. When t' is between 0 and 0.5, $O2^{i}$ is located near the center of the (M^{i},M^{x},M^{xi}) triangle, while $O2^{i}$ is close to the midpoint of M^{i}—M^{x} when t' is between 0.5 and 0.65. In the latter t' range, $O2^{i}$ is closest to M^{i} (Fig. 5). Similarly, $O2^{ii}$ near the midpoint of M^{i}—M^{ii} around $0.35 < t' < 0.5$ gives the M^{i}—$O2^{ii}$ distance less than 1.8 Å. Thus, when the O2 atom stays near the midpoint of the two M sites, the M—O2 distance becomes so short as to cause BVS higher than 4. As the M^{i}—M^{x} distance is 3.36 Å in the fundamental structure, the O2 atom just on the midpoint of M^{i}—M^{x} is only at 1.68 Å from the two metal sites. In the modulated structure, the M sites are displaced so as to keep the distance from the $O2^{i}$ longer than 1.78 Å, although the value is still too short. Refinements with higher Fourier terms, which may improve M—O2 distances, were unsuccessful, as mentioned in §3. A more effective way to prevent short M—O2 interactions is to modify modulation functions $x(t)$ and $y(t)$ of the O2 so as to discontinuously change at $t = 0.25$ and 0.75. (Note that $t' = -\sigma_2 t + y_0$ for $O2^{i}$ and $t' = -\sigma_2 t + y_0 + (1 - \sigma_2)/2$ for $O2^{ii}$, $y_0 = 0.25$.) If simple modulation functions in Figs. 8(*a*) and (*b*) are assumed, the $O2^{i}$ atom stays around the center of the (M^{i},M^{x},M^{xi}) triangle for a certain range of t' and jumps to positions within the neighboring triangles at $t' = -0.076$ and 0.576, as shown in Fig. 8(*c*). In this model, O2—O2 distances are always longer than 2.3 Å and M—O2 distances exceed 1.8 Å without modulations of the M site. Actual modulation functions of the O2 might be intermediate ones between those in Fig. 1 and Fig. 8. It seems, however, difficult to obtain precise modulation functions of

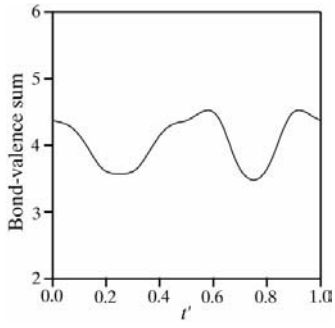

Figure 6
Bond-valence sum at the M site as a function of t' ($= -\sigma_2 x_2 + x_4$).

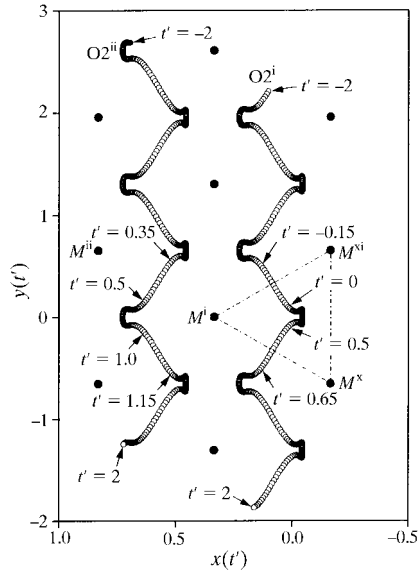

Figure 7
Trajectories of O2 atoms as functions of t' ($= -\sigma_2 x_2 + x_4$). Symmetry operations are (i) x_1, x_2, x_3, x_4; (ii) $x_1 + \frac{1}{2}, x_2 + \frac{1}{2}, x_3, x_4 + \frac{1}{2}$; (x) $x_1 - \frac{1}{2}, x_2 - \frac{1}{2}, x_3, x_4 - \frac{1}{2}$; (xi) $x_1 - \frac{1}{2}, x_2 + \frac{1}{2}, x_3, x_4 - \frac{1}{2}$.

the O2 atom from least-squares refinements because of the weak scattering ability of the O2 compared with those of the other species in the crystal.

In summary, as the refined structure contains rather uncommon geometries in parts, more extended studies are necessary for the complete understanding of this modulated structure. The present study, however, provides us with some basic features of the M—O2 plane which were unknown from previous studies.

(i) As a fundamental structure, O2 atoms are arranged with the shorter period along **b** rather than that of the triangular lattice of M, and construct a different subsystem from the rest of the crystal.

(ii) The O2 atom suffers such strong displacive modulations as to be significantly concentrated near the centers of the triangles of the M sites, reducing repulsive interactions from metal ions at the M sites.

(iii) The environment around the M site is varied from five to six coordination according to the modulation, which is associated with the occupational ordering of Fe and Ti at the site. The Fe ratio is relatively high at five-coordination sites, while six-coordination sites are mostly occupied by Ti atoms.

An assumption of no vacancies at metal positions leads to a relation between the chemical composition and the b_1^*/b_2^* ratio, that is σ_2 in the σ vector. The parameter x in the formula $InFe_{1-x}Ti_xO_{3+x/2}$ gives the expected value $\sigma_2 = 1 + x/2$. Actually, σ_2 estimated from the polycrystalline sample of $x = 2/3$ is given by the above relation, 1.33 (Brown, Flores *et al.*, 1999). [Note that q in previous papers (Brown, Flores *et al.*, 1999; Brown, Kimizuka *et al.*, 1999) is to be converted to σ_2 (= 1 + q).] The tendency is just as expected; the smaller x, the smaller σ_2, but the variation of observations from expected values is significant for compositions away from $x = 2/3$: $\sigma_2 = 1.281$ for $x = 8/15$. The relation is violated probably because the samples (single crystals and polycrystalline samples) have some kind of defect; the vacancy at the M and/or In site, the substitution of Fe and/or Ti for In *etc*. The present analysis considering vacancies at the M site can be one of the examples, although more complicated mechanisms may be necessary for polycrystalline samples. Superspace-group analysis of another structure type, the pseudorhombohedral form, is also planned.

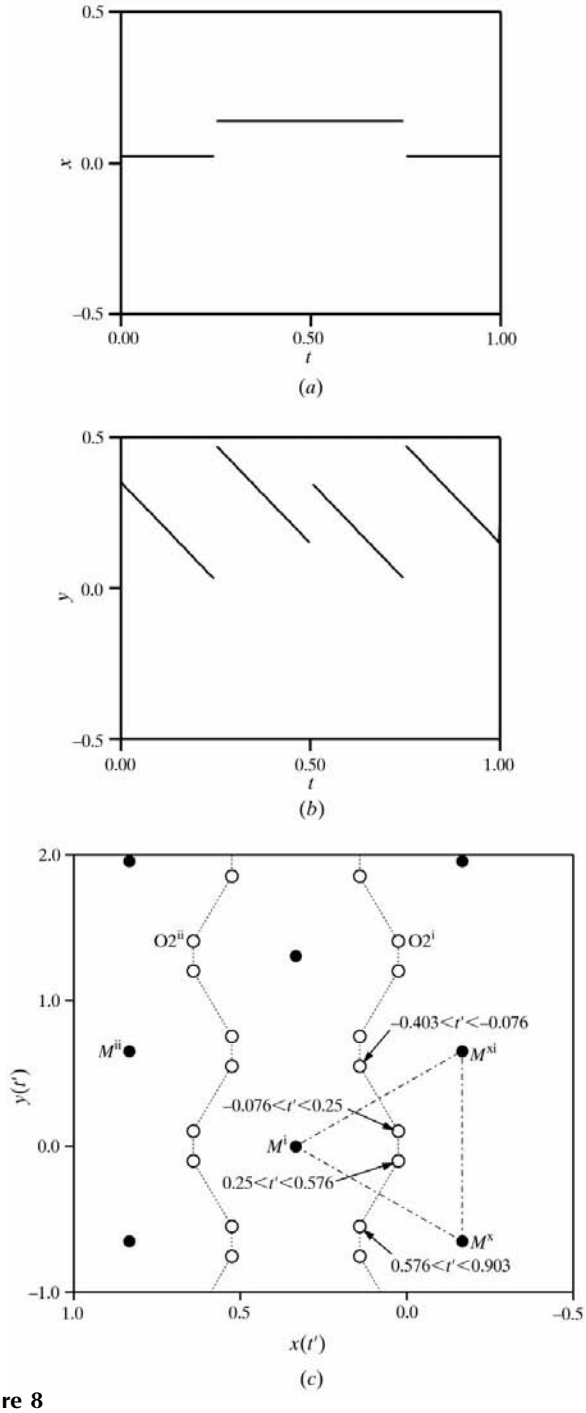

Figure 8
Model functions of the displacive modulation for (*a*) x, (*b*) y of the O2 atom and (*c*) the derived structure. Symmetry operations are (i) x_1, x_2, x_3, x_4; (ii) $x_1 + \frac{1}{2}, x_2 + \frac{1}{2}, x_3, x_4 + \frac{1}{2}$; (x) $x_1 - \frac{1}{2}, x_2 - \frac{1}{2}, x_3, x_4 - \frac{1}{2}$; (xi) $x_1 - \frac{1}{2}, x_2 + \frac{1}{2}, x_3, x_4 - \frac{1}{2}$.

The authors are grateful to Dr Akiji Yamamoto at AML/NIMS for helpful discussion about the refinement and Mr Kosuke Kosuda at AML/NIMS for the EPMA measurement.

References

Brown, F., Flores, M. J. R., Kimizuka, N., Michiue, Y., Onoda, M., Mohri, T., Nakamura, M. & Ishizawa, N. (1999). *J. Solid State Chem.* **144**, 91–99.
Brown, F., Kimizuka, N. & Michiue, Y. (2001). *J. Solid State Chem.* **157**, 13–22.
Brown, F., Kimizuka, N., Michiue, Y., Mohri, T., Nakamura, M., Orita, M. & Morita, K. (1999). *J. Solid State Chem.* **147**, 438–449.
Brown, I. D. & Altermatt, D. (1985). *Acta Cryst.* B**41**, 244–247.
Giaquinta, D. M., Davis, W. M. & zur Loye, H.-C. (1994). *Acta Cryst.* C**50**, 5–7.
Guillen, M. & Bertaut, E. F. (1966). *C. R. Acad. Sci. Paris Ser. B*, **262**, 962–965.
Janner, A. & Janssen, T. (1980). *Acta Cryst.* A**36**, 408–415.
Janssen, T., Janner, A., Looijenga-Vos, A. & de Wolff, P. M. (1999). *International Tables for Crystallography*, Vol. C, edited by A. J. Wilson, pp. 899–947. Dordrecht: Kluwer Academic Publishers.

Kato, K. & Onoda, M. (1991). *Acta Cryst.* A**47**, 448–449.
Kato, K. & Onoda, M. (1992). *Acta Cryst.* A**48**, 73–76.
Kato, K. & Tamura, S. (1975). *Acta Cryst.* B**31**, 673–677.
Kimizuka, N., Brown, F., Flores, M. J. R., Nakamura, M., Michiue, Y. & Mohri, T. (2000). *J. Solid State Chem.* **150**, 276–280.
Michiue, Y., Brown, F., Kimizuka, N., Onoda, M., Nakamura, M., Watanabe, M., Orita, M. & Ohta, H. (2000). *Chem. Mater.* **12**, 2244–2249.
Michiue, Y., Brown, F., Kimizuka, N., Watanabe, M., Orita, M. & Ohta, H. (1999). *Acta Cryst.* C**55**, 1755–1757.
Prewitt, C., Shannon, R. D. & Rogers, D. (1971). *Inorg. Chem.* **10**, 719–723.
Senegas, J., Manaud, J.-P. & Galy, J. (1975). *Acta Cryst.* B**31**, 1614–1618.
Shannon, R. D. (1976). *Acta Cryst.* A**32**, 751–767.
Yamamoto, A. (1992). *Acta Cryst.* A**48**, 476–483.